

RESEARCH ARTICLE

OPEN ACCESS

Synthesis Of Cobalt Doped Titania Nano Materials Assisted By Anionic Heterogemini Surfactants: Characterization And Its Applications In Heterogeneous Photocatalysis And Antibacterial Activity.

Radha Devi Chekuri, Siva Rao Tirukkovalluri^(*)

Department of Inorganic and Analytical Chemistry

School of Chemistry, Andhra University, Visakhapatnam, India.

*Corresponding Author: Sivarao Tirukkovalluri

Abstract: This paper presents about the synthesis of (0.25-1.0) wt.% cobalt doped titania nanomaterials without surfactants: pure $\text{Co}^{2+}/\text{TiO}_2$ and in presence of 1,4-Butane sultone and 1,3-Propane sultone Anionic Gemini surfactants and CTAB (Heterogemini surfactant)-0.5wt.% $\text{Co}^{2+}/\text{TiO}_2$ -HgS(1&2). The synthesized nano photocatalysts have been characterized by using various advanced techniques like X-Ray Diffraction (XRD), Ultraviolet-visible Diffuse Reflection Spectroscopy (UV-Vis DRS), X-ray Photoelectron Spectroscopy (XPS), Scanning Electron Microscopy (SEM), Energy Dispersive Spectrometry (EDS), Fourier Transform Infrared Spectroscopic Studies (FT-IR), Transmission Electron Microscopy (TEM). From the characterization studies all the catalysts synthesized were reported in anatase phase. TEM indicates the particles size of prepared catalysts reported with 7-10 nm and 15 nm for pure $\text{Co}^{2+}/\text{TiO}_2$ catalyst. From XPS studies Cobalt was found to be in +2 oxidation state. From BET results the surface area was reported to be 89.51 and 77.93 (m^2/g) for $\text{Co}^{2+}/\text{TiO}_2$ -HgS(1)& $\text{Co}^{2+}/\text{TiO}_2$ -HgS(2). From UV-DRS studies absorbance band shifted more towards visible region (red shift). In order to find out the efficiency of the synthesized photocatalyst the photocatalytic activity studies were carried out by degradation of Acid Red as a model azo dye pollutant in presence of the visible light irradiation. The antibacterial activity of the synthesized catalysts against Escherichia coli was also studied. Thus from the results 0.5wt.% $\text{Co}^{2+}/\text{TiO}_2$ -HgS(1) exhibited highest photocatalytic activity for the degradation of azo dye Acid Red as well as proved to be an excellent antibacterial agent.

Keywords: Cobalt doped Titania nano photocatalysts, Anionic Heterogemini surfactants, sol-gel method, Photocatalytic degradation, Azo dyes, Acid Red

I. INTRODUCTION

Heterogeneous Photocatalysis is found to be the most promising technology used for wastewater treatment for the degradation of toxic contaminants like azo dyes especially from textile industries [1,2]. Some of the limitations of TiO_2 include its high band gap ($E_{bg} = 3.2 \text{ eV}$), and it can be excited only by UV light ($\lambda < 387 \text{ nm}$). The high rate of electron-hole recombination, within nano seconds, at TiO_2 particles results in a low efficiency of Photocatalysis [3]. In order to rectify these defects doping of metal ions [4] and non-metal ions into titania crystal lattice [5] has been preferred. From the literature there were very few reports on the synthesis of doping of Cobalt into titania. The photocatalytic activity of nominal composition $(\text{Ti}_{1-x}\text{Co}_x)\text{O}_{2-\delta}$ with $0.001 \leq x \leq 0.05$ were prepared via a sol-gel technique followed by air firing (200–1000 °C) [6]. The efficiency of the catalyst depends on particle size, shape and specific surface area. Recently Gemini surfactants are new group of surfactants superior to monomeric surfactants [7,8]. We have synthesized $\text{Co}^{2+}/\text{TiO}_2$ in presence of conventional surfactants in our

previous work. Our main aim is to investigate the effect of various surfactants on the synthesis of $\text{Co}^{2+}/\text{TiO}_2$ and hence we preferred Anionic Heterogemini surfactant Template. We have mainly focused on 2 significant factors like synthesis of $\text{Co}^{2+}/\text{TiO}_2$ nanomaterials with much reduction in particle size by employing Heterogemini surfactants by adopting solgel method and to study about the photo catalytic activity of the synthesized catalysts by degradation of Acid Red, an azo dye in presence of visible light. Though there are many methods like Hydrothermal method [9], Impregnation method [10]. We preferred sol-gel method for the synthesis of $\text{Co}^{2+}/\text{TiO}_2$ nanomaterials. Sultones are cyclic esters of sulphonic acids [11,12]. The synthesized $\text{Co}^{2+}/\text{TiO}_2$ - HgS-(1&2) nano materials are characterized by XRD, XPS, SEM, EDS, TEM, FT-IR, UV-vis DRS and BET analysis. The photocatalytic activity studies were investigated by considering Acid Red (AR) as dye pollutant in the presence of the visible light. Various parameters like effect of dosage of the catalyst, dopant concentration, pH of the solution, and

concentration of the dye were studied in later investigations.

II. EXPERIMENTAL PROCEDURE

2.1: Materials

Titanium tetra-n-butoxide [$\text{Ti}(\text{O}-\text{Bu})_4$], Cobalt Nitrate were obtained from E. Merck (Germany), were used as titanium, Cobalt and sources for preparing $\text{Co}^{2+}/\text{TiO}_2$ photocatalysts. 1,4-Butane Sultone and 1,3-Propane Sultone Anionic Gemini surfactants were obtained from Sigma Aldrich (Germany). Acid Red 249 was used as model pollutant (India, analytical grade) for degradation.

2.2. Synthesis of Cobalt doped TiO_2 assisted by Heterogemini surfactants

In the present synthesis titanium tetra-butoxide and cobalt nitrate were taken as precursors for the preparation of $\text{Co}^{2+}/\text{TiO}_2$ nano materials synthesized in presence of Heterogemini surfactants. $\text{Co}^{2+}/\text{TiO}_2$ photocatalysts were synthesized in presence of 1,4-Butane sultone and 1,3-Propane sultone (under continuous stirring for 4h) and mentioned as Heterogemini surfactant HgS-(1). Similarly $\text{Co}^{2+}/\text{TiO}_2$ -HgS-(2) photocatalysts were synthesized by adding 1,4-Butane sultone Anionic Gemini surfactants and conventional cationic surfactant CTAB (under continuous stirring for 4h). Initially solution I was prepared by taking 21.0 ml of titanium tetra-butoxide in 40.0 ml of absolute alcohol with stirring for 10 min and then 3.0 ml of Nitric acid was added drop wise under continuous stirring for 30 min. Solution II containing 1.1715 g of Cobalt nitrate with 40.0 ml of absolute ethanol (100%) and 7.1 ml of water with required percentages (0.5 wt % $\text{Co}^{2+}/\text{TiO}_2$) was prepared with continuous stirring. To this HgS-(1) surfactant solution is added and stirred vigorously. Solution II was added to Solution I slowly and pH is maintained at 8, with continuous stirring at room temperature until the transparent sol was obtained. The resulting sol was stirred for 2 h and was aged at 25°C for 48 h. The gel was dried at 110°C in an oven for 36 h. The Catalyst powder was calcined at 450°C in a furnace for 4 h. The synthesis pattern has been given in Fig.1. $\text{Co}^{2+}/\text{TiO}_2$ -HgS(2) is also synthesized by adopting the same procedure and by adding HgS-(2) surfactant to Solution II. A pure cobalt doped TiO_2 (anatase) sample was also prepared by adopting the above procedure without adding the surfactant medium. The powders were used for XRD analysis, UV-visible absorption studies, XPS, SEM, TEM, DRS and FT-IR studies and for photocatalytic activity testing.

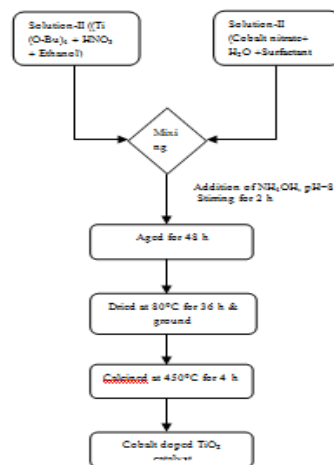


Fig.1.Schematic representation of synthesis of the catalyst in presence of Hetero Gemini Surfactant.

2.3 Characterization of Cobalt doped titania nano materials.

The XRD patterns were recorded with a Bruker AXS D8 advance diffractometer at room temperature with a copper ($\text{K}\alpha$) anode material of wavelength (λ) 1.5406 Å, and carbon monochromator were used. The UV–Visible absorption spectroscopic analysis of the catalysts was done by using a UV–Vis- spectrophotometer (Varian, carry5000). X-ray photo electron spectroscopy (XPS) of the prepared undoped and doped TiO_2 solid samples were recorded with auger electron spectroscopy (AES) module PHI 5000 Versa Prob II, FEI Inc. For SEM of the samples JEOL Model JSM - 6390LV was used. IR spectra of the synthesized samples were recorded on Thermo Nicolet Nexus 670 Spectrometer, with resolution of 4 cm^{-1} in KBr pellets. TEM measurements were carried out using Jeol/JEM 2100, operated at 200 kV as accelerating. The BET surface area was determined from the N_2 adsorption-desorption isotherm at 77.3 K by using a Autosorb I; Quantachrome Corp. system.

2.4 Photocatalytic activity of the catalyst - Degradation of AR:

The photocatalytic degradation of AR dye was carried out in presence of visible light in the photo catalytic reactor. The suspensions were then irradiated under visible light using a UV filtered Osram high pressure mercury vapour lamp with power 400W and 35000 lum. The quantitative determination of AR was performed by measuring the absorption of solution with Milton Roy Spectronic 1201, UV-Vis spectrophotometer. The

extent of AR photo catalytic degradation was calculated using a calibrated relationship between the measured absorbance and its concentration. AR cannot be photodegraded in the absence of the catalyst under the same irradiation conditions.

$$\% \text{ of the Degradation} = (A_0 - A_t) / A_0 \times 100 \%$$

Where A_0 = Initial absorbance of dye solution

A_t = Absorbance of dye solution at time t.

III. RESULTS AND DISCUSSION

3.1. X-ray diffraction studies:

The XRD patterns for all the synthesized 4 photocatalysts, pure TiO_2 , 0.5 wt.% pure $\text{Co}^{2+}/\text{TiO}_2$, and 0.5 wt.% $\text{Co}^{2+}/\text{TiO}_2-\text{HgS}(1)$ and 0.5 wt.% $\text{Co}^{2+}/\text{TiO}_2-\text{HgS}(2)$ were shown in Fig.2.(a to d). All the samples were reported in the anatase phase. (JCPDS File number: 15-0923). The highest intensity peak was observed for $\text{Co}^{2+}/\text{TiO}_2-\text{HgS}(1)$ observed at $2\theta = 25.1^\circ$. Thus particle size was calculated by using Scherrer's equation[13] where the particle size was found to be ranging from 7.42 - 9.56nm. These values are shown in Table 2.

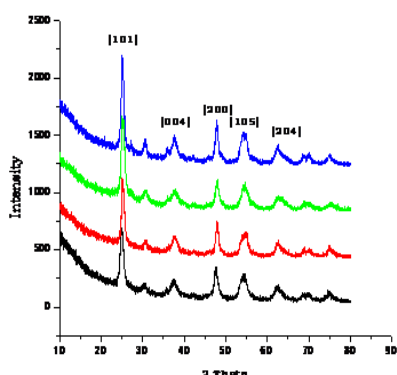


Fig.2 XRD patterns of (a)pure TiO_2 ,(b) 0.5wt.% pure $\text{Co}^{2+}/\text{TiO}_2$ (c) 0.5wt.% $\text{Co}^{2+}/\text{TiO}_2-\text{HgS}(1)$ and (d). 0.5 wt. % of $\text{Co}^{2+}/\text{TiO}_2-\text{HgS}(2)$.

3.2. UV–Visible Diffuse Reflectance Spectroscopy:

The UV–Visible diffuse reflectance spectra of the synthesized samples of pure 0.5wt.% $\text{Co}^{2+}/\text{TiO}_2$ nanophotocatalysts synthesized in presence of 2 different surfactants were given in Fig.3. There was shift observed towards higher visible region (red shift). Due to doping of Cobalt into titania decrease in band gap energy was observed. Band gap Energy for the synthesized catalysts have been calculated by using the formula $E_g = (1240/\lambda)$, where E_g is band gap, λ is the wavelength and the values are presented in Table 1. Due to this red shift there is more generation of electron/hole pairs that could be excited with less

energy which makes the catalyst more efficient towards photocatalytic activity which was evidenced from the later studies.[14]

Table1. Band gap energy calculated for synthesized photocatalysts

Catalyst	Band gap energy (ev)
Pure TiO_2	3.2
Pure $\text{Co}^{2+}/\text{TiO}_2$	2.98
$\text{Co}^{2+}/\text{TiO}_2-\text{GS}$	2.5
$\text{Co}^{2+}/\text{TiO}_2-\text{HGS}(1)$	2.55
$\text{Co}^{2+}/\text{TiO}_2-\text{HGS}(2)$	2.65

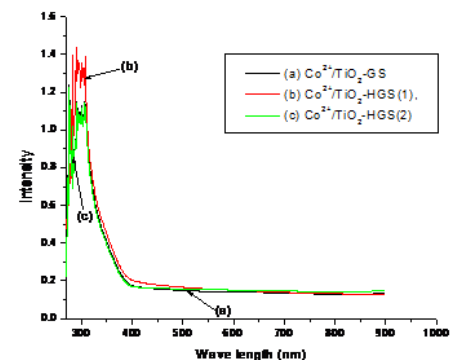


Fig.3. UV–Visible absorption spectra of (a) 0.5wt. % of $\text{Co}^{2+}/\text{TiO}_2-\text{GS}$
(b) 0.5wt.% of $\text{Co}^{2+}/\text{TiO}_2-\text{HgS}(1)$, (c) 0.5wt.% of $\text{Co}^{2+}/\text{TiO}_2-\text{HgS}(2)$

3.3. X-ray photoelectron spectroscopic study:

From X-ray photoelectron spectroscopic analysis chemical state information of Co 2p, O 1 s, and Ti 2p and their oxidation states was known. Fig.4. (a-c) shows High resolution XPS Ti 2p, O 2p, Co 2p spectrum of 0.5wt% of $\text{Co}^{2+}/\text{TiO}_2-\text{HgS}(1)$. Fig.4. (a) indicates the binding energies of $\text{Ti } 2p_{3/2}$ and $\text{Ti } 2p_{1/2}$ and were found to be 458.01 eV and 463.9 eV, these binding energies belongs to Ti^{4+} and differ slightly due to the pulling of $\text{Ti}-\text{O}-\text{Ti}$ bond. The Ti 2p and O 1 s peaks of $\text{Co}^{2+}/\text{TiO}_2$ samples are slightly shifted towards higher binding energy, when compared to that of pure TiO_2 which has binding energy of 458.3eV. This is due to incorporation of Co^{2+} ions into TiO_2 lattice. Fig. 4(c) shows the high resolutions XPS Spectra of Co are present in the state of +2 oxidation state. From Fig.4(c) $\text{Co } 2p_{3/2}$ and $\text{Co } 2p_{1/2}$ peaks were located at binding energies of 779.9 and 782 eV respectively, and they belong to Co [15-18] and shake-up peaks are also observed which are characteristic for Co^{2+}

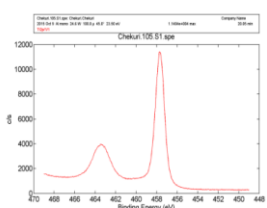


Fig.4. (a) High resolution XPS Ti 2p spectrum of 0.5wt% of $\text{Co}^{2+}/\text{TiO}_2$ HgS (1)

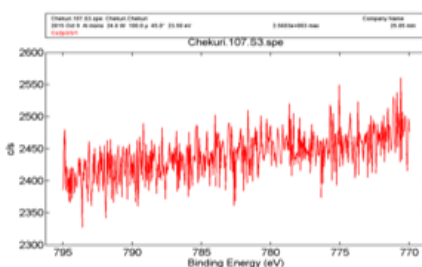


Fig.4. (c) High resolution XPS Co 2p spectrum of 0.5wt% of $\text{Co}^{2+}/\text{TiO}_2$ - HgS (1)

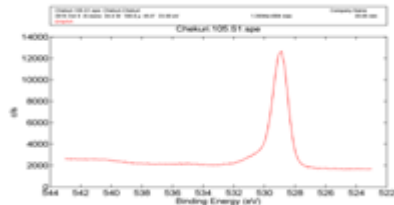


Fig.4. (b) High resolution XPS O 2p spectrum of 0.5wt% of $\text{Co}^{2+}/\text{TiO}_2$ -HgS(1)

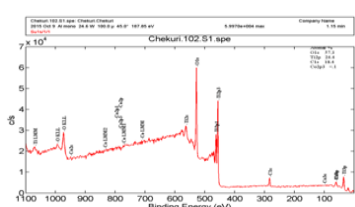


Fig.4. (d) Total Survey spectrum of 0.5wt% of $\text{Co}^{2+}/\text{TiO}_2$ HgS(1)

3.4 Scanning electron microscopic study:

SEM micrographs indicate the change in morphology of the synthesized catalysts. Fig.5 depicts the SEM micrograph of 0.5wt. % $\text{Co}^{2+}/\text{TiO}_2$ -HgS(1). Fig.6 represents the SEM micrographs of 0.5wt.% $\text{Co}^{2+}/\text{TiO}_2$ -HgS (2). Fig.6 shows large number of tiny globular nanoparticles, with reduction in the particle size when compared to that of pure TiO_2 . SEM indicates the change in the morphology of the nanoparticles, with enlarged surface area without any agglomeration of the particles. This indicates the role played by surfactant involved during the synthesis of the catalyst. Presence of surfactant leads to encapsulation of the doped titania due to which particle size is restricted from further growth leading to synthesis of particles with much reduction.

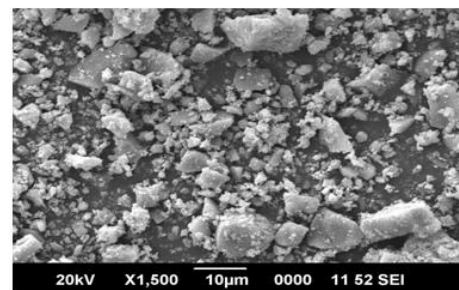


Fig.5 SEM micrograph of 0.5wt. % $\text{Co}^{2+}/\text{TiO}_2$ -HgS(1).

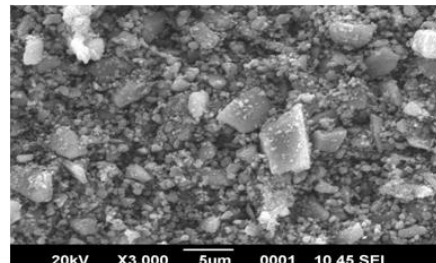


Fig.6 SEM micrograph of 0.5wt.% $\text{Co}^{2+}/\text{TiO}_2$ HgS(2).

3.5 Fourier transform infrared spectroscopy:

Fig. 7(a) & (b) indicates FT-IR images of 0.5 wt. % Co^{2+} / TiO_2 -HgS(1), after and before calcinations. From Fig7 (b) bands were noticed at 3383.56 and 1622.12 cm^{-1} which correspond to the stretching vibrations of the O-H and bending vibrations of the adsorbed water molecules. This confirms the presence of hydroxyl ions in the $\text{Co}^{2+}/\text{TiO}_2$. The Ti–O–Ti stretching peak appears at 602 – 559.67 cm^{-1} . This small deviation may be due to Co doped substitutionally in the TiO_2 matrix. Fig 7(b) peaks are located at 3134.64 , 1624.60 , 1400.20 , 1196.58 , 1138.14 cm^{-1} 1047.84 , and 983.78 cm^{-1} are due to the presence of surfactants

before calcinations. The absence of these bands in Fig.7 (a) confirms that there was no surfactant present in the synthesized catalyst after calcinations.

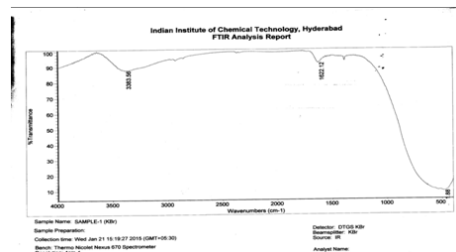


Fig. 7(a) indicates FT-IR images of 0.5 wt.% $\text{Co}^{2+}/\text{TiO}_2\text{-HgS}(1)$, after calcinations

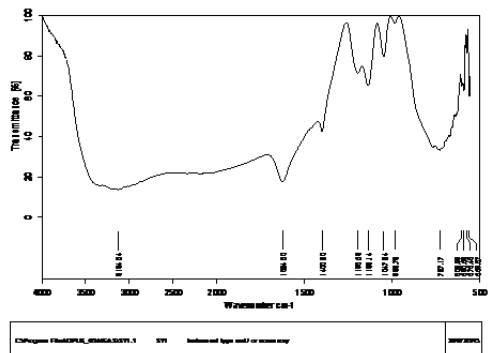


Fig.7(b) indicates FT-IR images of 0.5wt.% $\text{Co}^{2+}/\text{TiO}_2\text{-HgS}(1)$, before calcinations.

3.6. Transmission electron microscopy

Fig.8, Fig.9 and Fig.10 indicates HR TEM images of 0.5wt. % pure $\text{Co}^{2+}/\text{TiO}_2$ 0.5wt.% $\text{Co}^{2+}/\text{TiO}_2\text{-HgS}(1)$, 0.5wt.% of $\text{Co}^{2+}/\text{TiO}_2\text{-HgS}(2)$. The particle size was found to be 7-10 nm, while that of pure $\text{Co}^{2+}/\text{TiO}_2$ was reported to be 15 nm respectively. From TEM analysis we can conclude the decrease in the particle size, which signifies the effect of Heterogemini surfactant medium, which restricted the further growth of TiO_2 crystalline particles and thus played a vital role in synthesizing the particles with reduced size and with large surface area. This is due to encapsulation of the surfactant medium on the $\text{Co}^{2+}/\text{TiO}_2$ where particle size is restricted without any agglomeration. Where as in presence of

$\text{HgS}(2)$ particle size was of bigger size since encapsulation may not be formed effectively due to the introduction of CTAB with 1,4-Butane sultone. Due to synthesis of particles with minimum size and larger surface area which are the prominent factors for higher efficiency of the

synthesized catalyst hence the same result is observed from the later photocatalytic studies

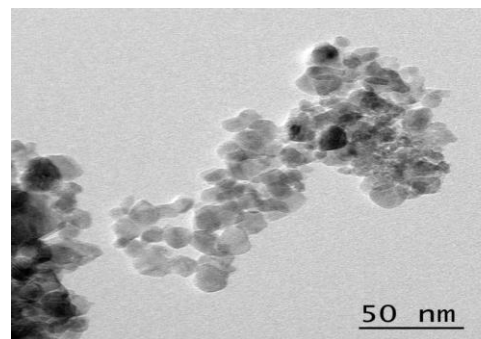


Fig.8 HR TEM images of pure Co^{2+}/Ti

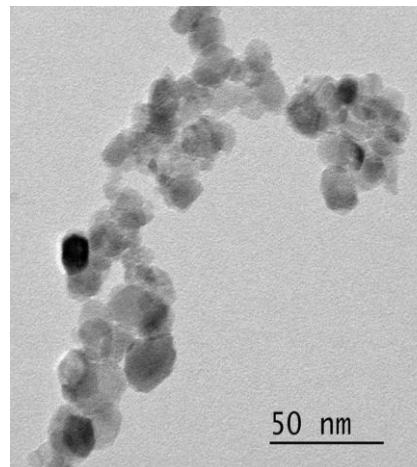


Fig.9 HR TEM images of $\text{Co}^{2+}/\text{TiO}_2\text{-HgS}(1)$

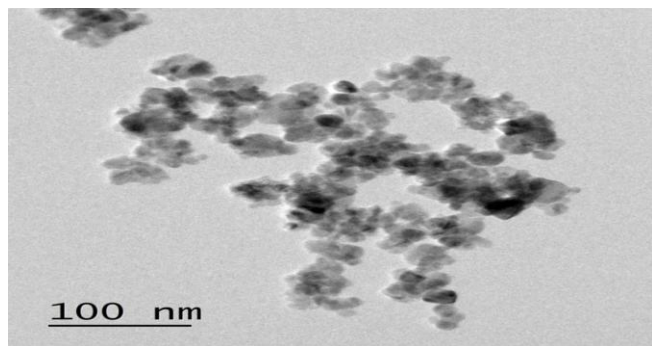


Fig.10.HR TEM images of 0.5wt. % of $\text{Co}^{2+}/\text{TiO}_2\text{-HgS}(2)$

3.7 BET Analysis:

From BET analysis Surface area A_{BET} (m^2/g) of the synthesized catalysts were represented in the Table 3. The surface area was reported to be-89.51 and 77.93 (m^2/g) for $\text{Co}^{2+}/\text{TiO}_2\text{-HgS}(1)$ & $\text{Co}^{2+}/\text{TiO}_2\text{-}$

HgS(2). These values are reported with higher values when compared to those reported from literature for synthesis of Cobalt doped titania [19,20] by employing different methods.

Table 2. BET analysis Surface area A_{BET} (m^2/g), results of the synthesized catalysts

Catalyst	A_{BET} (m^2/g)	Crystallite size(nm)
Pure Co^{2+}/TiO_2	26	13
$Co^{2+}/TiO_2-HgS(1)$	89.51	7.42
$Co^{2+}/TiO_2-HgS(2)$	77.93	9.56

3.8. Evaluation of Photocatalytic activity of the Co^{2+}/TiO_2-HgS

The photocatalytic activity studies of the synthesized catalyst, 0.5wt.% Co^{2+}/TiO_2-HgS (1) was determined by carrying out photocatalytic degradation of Acid Red (AR) an azo dye pollutant under visible light. Experiments were carried out to find the optimum conditions of various parameters like pH of the solution, catalyst dosage and concentration of the dye.

3.8.1. Effect of pH

Experiments were performed to find out the optimum conditions of pH by considering the dye concentration and weight of the catalyst as constant. The experimental results have been graphically expressed in Fig.11. From the Fig.11 it can be observed that the rate of degradation of the Acid Red dye was maximum at pH 5. The interaction between the semiconductor surface and the substrate and charged radicals mostly depend on the pH of the solution [21]. Acidic conditions favour the adsorption of the dye on the catalyst surface. Hence the optimum condition for Acidred dye is found to be at pH 5. The rate of degradation for 0.5 wt. % Co^{2+}/TiO_2 was found to be maximum at pH=5 is $3\text{ mg L}^{-1}\text{min}^{-1}$ for degradation of the Acid Red.

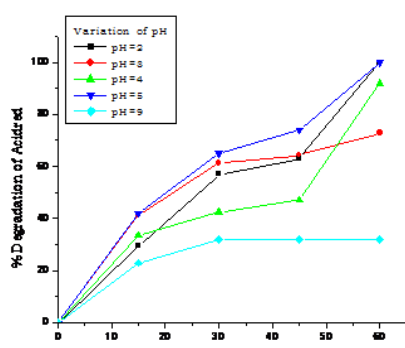


Fig.11. pH effect- degradation of Acid Red

3.8.2: Effect of catalyst dosage

In order to find the optimum catalyst dosage other conditions like pH and dye concentration are kept constant experiments were carried on by varying the amount of the synthesized $Co^{2+}/TiO_2-HgS(1)$ catalyst from 0.05 to 0.3 g in 100ml of Acidred dye solution. The experiments were carried on has been graphically expressed in Fig.12. From the Fig.12 it is observed that degradation of the dye is maximum at 0.1g and later with increase in weight there is decrease in the degradation. As the amount of the catalyst increases more number of photons is being absorbed which results in more generation of electron-hole pairs. This increases the number of hydroxyl radicals which is the main factor increasing the rate of photocatalytic degradation. With increase in catalyst dosage beyond 0.1g the photocatalytic activity was decreased, this is due to increase in turbidity of solution which restricts the light to penetrate through the solution. With increase in concentration of the catalyst due to aggregation of catalyst molecules also photocatalytic activity is decreased. The rate of degradation of 0.5 wt. % Co^{2+}/TiO_2 was found to be maximum at pH=5 is $3.55\text{ mg L}^{-1}\text{min}^{-1}$ for degradation of Acid Red.

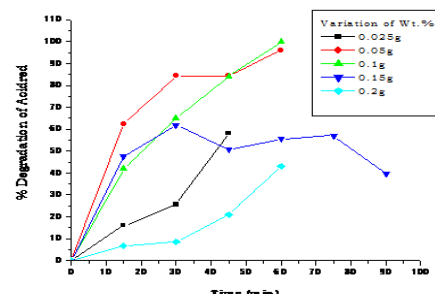


Fig.12. Effect of Catalyst dosage- degradation of Acid Red.

3.8.3: Effect of initial dye concentration;

In order to find out the optimum conditions for initial dye concentration experiments were carried on by changing the dye concentration from $1,5$ & 15 mg L^{-1} while keeping the other conditions constant. The experimental results have been graphically expressed in Fig.13. From the Fig.13 it is observed that the optimum initial dye concentration for maximum degradation of Acidred was observed at 5 mg L^{-1} and with further increase in dye concentration decrease in degradation rate was observed. Finally the optimum condition of initial dye concentration is found to be 5 mg L^{-1} . The rate of degradation of 0.5 wt. % Co^{2+}/TiO_2 was found to be maximum and is $4.7\text{ mg L}^{-1}\text{min}^{-1}$ for degradation of Acid Red.

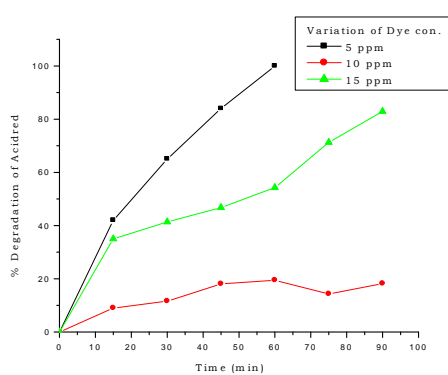
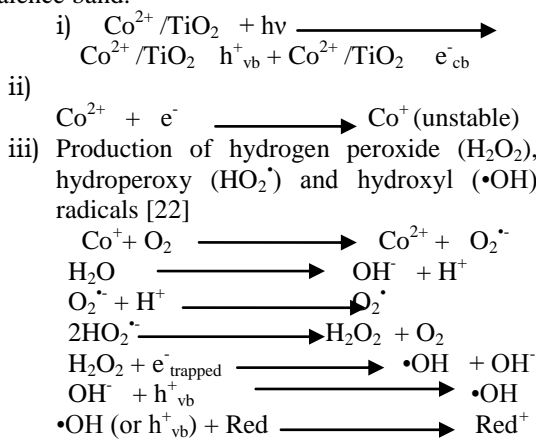


Fig.13.Effect of initial dye concentration-degradation of Acid Red.

Overall mechanism

The following mechanism is proposed for the photocatalytic reactions of $\text{Co}^{2+}/\text{TiO}_2-\text{HgS}$

(i).Generation of electrons and positive holes in the valence band.



Where 'Red' is the pollutant an electron donor (reductant).

Thus Acid Red is attacked by the hydroxyl radicals formed and results in the generation of organic radicals or other intermediates.

IV. PHOTOCATALYTIC ANTIBACTERIAL ACTIVITY OF THE SYNTHESIZED CATALYSTS:

The efficiency of the synthesized catalyst was evaluated by carrying out the antibacterial activity studies on Escherichia coli-Gram negative bacteria. E.coli (ATCC 8739) was selected as a target organism towards antibacterial activity studies.

4.1: Anti-bacterial studies:

The Nutrient agar medium was sterilized at 121°C at pressure of 15 lb for 20 min. The prepared nutrient broth was cultured in an incubator at 37 °C for 2 days. Required amount of

the $\text{Co}^{2+}/\text{TiO}_2$ photocatalyst was added to 9 mL of 0.9 % saline solution and it was sterilized by autoclaving at 120 and 15 lbs for 20 min. An aliquot of E.coli cell suspension (4.9mL) was pipetted out into a sterile petridish in a laminar airflow chamber. To the same petridish, 0.1mL of the photocatalytic nano powder suspension at a concentration of 1mg/10ml was added and exposed to the visible light irradiation. After appropriate dilutions in sterile water, aliquots of 1mL were spread on to agar plates and incubated at 37 °C for 24 hours. The numbers of viable cells in terms of colony forming units were counted. Growths of bacterial colonies were seen on these agar plates and were counted. Anti bacterial efficiency (in percent) was reported using the equation, $\{\text{Co} - \text{C}\} / \text{Co} \times 100 / \text{Co}$, where Co and C are the number of colonies formed before and after irradiation. Fig 14. Shows the colony forming units of E.coli after treatment with all the synthesized different $\text{Co}^{2+}/\text{TiO}_2-\text{HgS}$ (1) photocatalysts under visible light irradiation. It was observed that there is decrease in the no. of colonies in agar medium plates. Table-3 represents the % survival of E.coli after treatment with $\text{Co}^{2+}/\text{TiO}_2$ photocatalysts. Fig.15 shows graph plotted between the antibacterial efficiency of the catalysts against irradiation time. Almost complete elimination of bacterial colonies was observed within 60 min exposure. Bacterial cell wall is rigid and important for maintenance of cell. The outer membrane of E. coli is made of lipopolysaccharide which provides a strong network for the existence of cell [23,24].

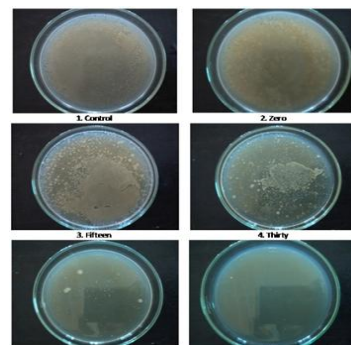


Fig.14. Colony forming units of E.coli after treatment with - 0.5wt% $\text{Co}^{2+}/\text{TiO}_2-\text{HgS}$ under visible light irradiation

Table: 3 The survival (%) of E.coli after treatment with 0.5wt. % pure $\text{Co}^{2+}/\text{TiO}_2-\text{HgS}$ (1)

Time	CFU	% of Bacterial survival
Control	1800	-
0	1780	100
15	1050	98.57
30	550	64.54
45	80	8.75
60	12	0

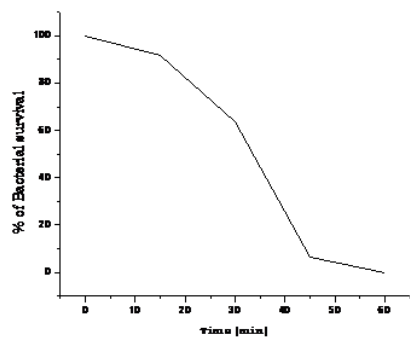


Fig.15 The survival (%) of E.coli after treatment with -0.5wt.% pure $\text{Co}^{2+}/\text{TiO}_2-\text{HgS}$ with time.

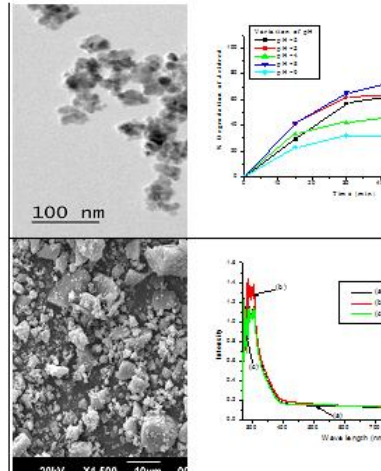
V. CONCLUSIONS:

In this paper we focussed on synthesis of Cobalt doped TiO_2 photocatalysts assisted by Heterogemini surfactants like (1-4Butane sultone, 1-3Propane sultone Anionic Gemini surfactants, CTAB) by using sol-gel technique. Acid Red, a model azo-dye pollutant has been selected for photocatalytic degradation by the synthesized $\text{Co}^{2+}/\text{TiO}_2-\text{HgS}$ (1).All the $\text{Co}^{2+}/\text{TiO}_2$ catalysts synthesized with surfactant medium were reported in anatase phase. From TEM analysis particle size of the synthesized 0.5wt. % $\text{Co}^{2+}/\text{TiO}_2-\text{HgS}$ (1&2) catalysts were reported in the range between 7-10 nm where as for pure 0.5wt. % $\text{Co}^{2+}/\text{TiO}_2$ it was reported to be 15nm. Due to doping of Cobalt into titania matrix shift in the absorption band towards visible light region (red shift) i.e., above 400-700 nm has been confirmed. XPS indicated the presence of cobalt in Co^{2+} oxidation state and as substituent dopant for Ti^{4+} in the TiO_2 matrix. BET analysis confirmed particle size with much increase in the surface area of the synthesized catalyst assisted with HgS (1) surfactant medium i.e. $89.51\text{m}^2/\text{g}$ when compared to pure $\text{Co}^{2+}/\text{TiO}_2$.This clearly signifies the effect of encapsulation on $\text{Co}^{2+}/\text{TiO}_2$ by various surfactants during the synthesis of the catalyst. From SEM micrographs of the catalysts no agglomeration is observed and the particles are spherical and homogeneous. From FT-IR analysis it is evident that Cobalt is doped substitutionally into the TiO_2 matrix. We can conclude that the entry of cobalt ion into TiO_2 lattice is substitutional with decrease in particle size and increased surface area with red

shift being observed towards visible light region. The optimum concentrations of various parameters include: Effect of dopant concentration (0.5 wt. %), pH Effect (pH-5), Catalyst dosage (0.1g) and Initial dye concentration ($5\text{mg} \cdot \text{L}^{-1}$). Thus the 0.5wt. % $\text{Co}^{2+}/\text{TiO}_2-\text{HgS}$ (1) has been proved to be an effective nano photocatalyst towards photocatalytic degradation of Acid Red, azo dye as well as an excellent antibacterial agent by studying against E.coli-Gram negative bacteria.

REFERENCES

- [1]. I.Oller., S.Malato, J.A. Sánchez-Pérez Combination of Advanced Oxidation Processes and biological treatments for wastewater decontamination-A review. Science of the Total Environment **409** (2011) 4141.
- [2]. D.Arsene, CP Musteret,C Catrinescu,P Apopei,G Barjoveanu , CTeodosiu. Combined oxidation and ultra filtration processes for the removal of priority Organic pollutants from wastewaters. Environmental Engineering and Management Journal **10** (2011) 1967.
- [3]. C.Kormann, D.W.Bahnemann and M.R.J.Hoffmann Phys. Chem., **92** (1988) 5196.
- [4]. M. Anpo and M.J.Takeuchi Catal., **216** (2003) 506.
- [5]. A. Hattori and H.J. Tada. Sol-gel Sci. Technol., **22** (2001) 47.
- [6]. Suo Hon Lim, Cristiano Ferraris, Martin Schreyer, Kaimin Shih, James, O. Leckie, T.J. White The influence of cobalt doping on photocatalytic nanotitania: Crystal chemistry and amorphicity Journal of Solid State Chemistry **180** (2007) 2905.
- [7]. R. Zana, Gemini Surfactants: Synthesis, Interfacial and Solution-Phase Behavior, and Applications, CRC Press (2003).
- [8]. R. Zana, in: Novel Surfactants: Preparation, Applications and Biodegradability, M. Dekker Inc, New York (1998).
- [9]. Mustafa, Chem. Rev., **54** (1954)195.
- [10]. Y.Oguri, R. E Riuan and H. K.Bowen J. Mater. Sci., **23** (1988) 2897.
- [11]. S.Sakthivel,M.VShankar,M.Palanichamy , B.Arabindoo, D. W Bahnemann and Murugesan V.Water Res., **38** (2004) 3001.
- [12]. Matsni and Sakurada, Mem. Coll. Sei Kyoto Imp. Univ. A15 Chem. Abstr. **26** (1932) 5264.

- [13]. E.D. Jeong, P. H.Borse, J.S.Jang, J.S. Lee, Ok-Sang Jung, H.Chang, J.S. Jin, M. S. Won and H.G. Kim, Hydrothermal synthesis of Cr and Fe co-doped TiO_2 nano particle photocatalyst, *J. Ceramic Processing Research*, **9** (2008) 250.
- [14]. C.Lettmann, K. Hildenbrand, H. Kisch, W. Macyk and W.F. Maier, *Appl. Catal. B Environ.* **32**, 2001, 215–227.
- [15]. G.Sadanandam,K.Lalitha,V.DurgaKumari, M.V.Shankar, M.Subrahmanyam, Cobalt doped TiO_2 : A stable and efficient photocatalyst for continuous hydrogen production from glycerol: Water mixtures under solar light irradiation, *International Journal of hydrogen energy* **38** (2013) 9655.
- [16]. H.J. Choi and M. Kang, Hydrogen production from methanol/water decomposition in a liquid photo system using the anatase structure of Cu loaded TiO_2 , *J. Hydrogen Energy* **32**, 2007, 3841–3848.
- [17]. Manoranjan sahu and Pratim Biswas, Single step processing of copper doped titania nano materials in a flame aerosol reactor , *Nanoscale research letters* **6** (2011) 441.
- [18]. Amadelli R, Samiolo L., Maldotti A, Molinari A, Valigi M, Gazzoli D, Preparation, characterization, and photocatalytic behavior of Co-TiO₂ with Visible light response, *International Journal of Photo energy*, 853, (2008) 753.
- [19]. Katarzyna Siwinska-Stefanska, Dominik Paukszta, Adam Piasecki, Teofil Jasionowski “Synthesis and physico chemical characteristics of titanium dioxide doped with selected metals”**50** (2014) 265.
- [20]. M.Hamadanian, A. Reisi-Vanani and A.Majedi Sol-Gel Preparation and Characterization of Co/TiO₂ Nanoparticles: Application to the Degradation of Methyl Orange J. Iran. Chem. Soc.,**7** (2010)S52.
- [21]. G.Marci , V.Augugliaro , A.Bianco Prevot, C.Baiocchi , E.Garcia-Lopez , V.Loddo, L.Palmisano , E.Pramauro and M.Schiavello, *Annali di Chimica by Societa Chimica Italiana*, **93** (2003) 639–645.
- [22]. T. Wu, T. Lin, J. Zhao, H. Hidaka and N. Serpone, *Environ. Sci. Technol.* **33**, 1999, 1379-1387.
- [23]. Suja Devipriya “Semiconductor oxide mediated photocatalytic removal of chemical and bacterial pollutants from wastewater” Ph.D thesis (2006).
- [24]. Y.S.Yang, G.Wang ,Y.H.Shen, Microbial Physiology, Chemical Industry (2007) 10.
- 
- The figure consists of three panels. The top panel is a Transmission Electron Microscopy (TEM) image showing a collection of small, irregularly shaped particles. A scale bar indicates 100 nm. The middle panel is a line graph titled "Variation of % Degradation" versus "Time (min)". The y-axis ranges from 0 to 100, and the x-axis ranges from 0 to 45. Four curves are plotted: (a) black line with circles, (b) red line with squares, (c) green line with triangles, and (d) blue line with crosses. All curves show an increase in degradation percentage over time, with curve (a) reaching the highest percentage. The bottom panel is a UV-vis Diffuse Reflectance Spectroscopy (DRS) plot showing Intensity versus Wavelength (nm). The x-axis ranges from 200 to 800 nm, and the y-axis ranges from 0.0 to 1.0. Three curves are shown: (a) black curve peaking at ~350 nm, (b) red curve peaking at ~350 nm, and (c) green curve peaking at ~350 nm. All curves show a significant decrease in intensity as wavelength increases beyond 400 nm.